Iterative Channel Estimation for MIMO-OFDM System in Fast Time-Varying Channels

Lihua Yang, Longxiang Yang, Yan Liang
Jiangsu Key Laboratory of Wireless Communication, Nanjing University of Posts and Telecommunications, Nanjing, Jiangsu 210003, China
[e-mail: yanglh@njupt.edu.cn; yanglx@njupt.edu.cn; liangyan@njupt.edu.cn]
*Corresponding author: Lihua Yang

Received March 21, 2016; revised June 28, 2016; accepted July 16, 2016; published September 30, 2016

Abstract

A practical iterative channel estimation technique is proposed for the multiple-input-multiple-output orthogonal frequency division multiplexing (MIMO-OFDM) system in the high-speed mobile environment, such as high speed railway scenario. In the iterative algorithm, the Kalman filter and data detection are jointed to estimate the time-varying channel, where the detection error is considered as part of the noise in the Kalman recursion in each iteration to reduce the effect of the detection error propagation. Moreover, the employed Kalman filter is from the canonical state space model, which does not include the parameters of the autoregressive (AR) model, so the proposed method does not need to estimate the parameters of AR model, whose accuracy affects the convergence speed. Simulation results show that the proposed method is robust to the fast time-varying channel, and it can obtain more gains compared with the available methods.

Keywords: MIMO-OFDM, high-speed mobile, fast time-varying channel, iterative channel estimation, Kalman filter, data detection error.

This work was supported in part by 973 Program of China (2013CB329104), and 863 Program of China (2014AA01A705), the National Natural Science Foundation of China (61401232, 61501254), Natural Science Foundation of the Jiangsu Higher Education Institutions of China (14KJB510026), and Nanjing University of Posts and Telecommunications Project (NY213013).

http://dx.doi.org/10.3837/tiis.2016.09.012 **ISSN : 1976-7277**

1. Introduction

Orthogonal frequency division multiplexing (OFDM) system has the high frequency utilization efficiency and the strong multipath resistance. Meanwhile, the multiple-input-multiple-output (MIMO) can provide higher data rates by using parallel channels established in spatial domain over the same time and frequency without extra bandwidth. Thus, the MIMO-OFDM system that combines the advantages of the OFDM and MIMO has been considered as a key technology for the fourth generation wireless communication systems, and it has been employed in many practical applications [1].

Since the channel state information is required for the diversity combining, detection, precoding, and the spectrum sharing [2] etc., the channel estimation is essential for the MIMO-OFDM system to bring out the advantages of the MIMO-OFDM. Currently, the various channel estimation schemes have been presented for the MIMO-OFDM system [3]-[5], the most of which are based on the assumption of the quasi-static or slow time-varying fading channel within a MIMO-OFDM block. However, the assumption is invalid in the high speed mobile scenario, such as high speed railway, and the estimation errors by those techniques will be too high to be used in the equalization. In the high speed mobile environment, the variation of the channel introduces the intercarrier interference (ICI) during one OFDM symbol period, which is consequently becoming a serious challenge for the MIMO-OFDM system [6]-[7]. Therefore, the time-variation of channel within a block must be considered to support the high speed mobile channels.

In the high speed mobile scenario, many time-varying channel estimation techniques have been presented for the mobile MIMO-OFDM system [8]-[12]. Among these schemes in [8]-[10], the Kalman filter theory based the MIMO-OFDM channel estimation algorithms have been discussed and are effective methods because they can track the change of the channel gain in the high speed scenario. In [11], a dynamic autoregressive (AR)-model based channel prediction is used to the interference alignment. However, in these algorithms [8]-[11], the parameters of the AR system need to be estimated, and it is difficult to accurately decide the parameters of the AR model due to the model depending on the mobile speed, which affects the accuracy of the channel estimation or prediction. Literature [12] gives a practical MIMO-OFDM channel estimation method only using the Kalman filter without the parameter estimation of AR model. However, the scheme in [12] is only appropriate for the pilots in the frequency domain, and it cannot obtain the channel estimation of the data subcarriers with the high accuracy because the ICI caused by the time-varying channel is not considered.

Another line of research to improve the performance of the channel estimation is to consider the pilot design and channel estimation jointly [13]-[14]. Literature [13] gives a compressed sensing (CS) based channel estimation method, which improves the estimation accuracy by designing the pilot pattern to reduce the system coherence. In [14], a new data frame structure is presented to conveniently estimate the time-varying channel for the two-way relay networks. However, for the fixed frame structure, such as LTE system, these schemes will be unsuitable. Therefore, a time-varying channel estimation algorithm without changing the frame structure is desired in the high speed mobile MIMO-OFDM system.

Recently, some iterative algorithms joint channel estimation and data detection have been discussed in [15]-[17]. It is the iterative interaction between the channel estimation and the data detection to provide significant improvement compared with the non-iterative schemes.

However, the detection error in these iterative algorithms is inevitable, which will result in an error floor due to the dominance of the error propagation. Therefore, it is necessary to take into account these errors in the interaction to improve the estimation accuracy of the iterative schemes. Although the detection error is considered in [18], it has a slow convergence speed due to the effect of the estimated parameters of the AR model and the covariance of the modeling error.

In our previous works, we also give some time-varying channel estimation methods for the high speed mobile scenario [19]-[20]. These algorithms are presented for the TDD-LTE SC-FDMA system with the specific subframe pattern, so they are not appropriate for the other systems due to the different frame structures. Since the considered channel model is the line-of-sight (LOS) component dominant Rician channel in our previous works, the previous schemes ignores the intercarrier interference (ICI) caused by the time-varying channel during one SC-FDMA symbol period. Therefore, these algorithms in [19]-[20] have some limitations in terms of applicability.

To solve the above problems, we propose a practical iterative channel estimation algorithm for the high speed mobile MIMO-OFDM system in the paper. Specifically, the time-variation of the channel is firstly approximated by the polynomial-basis expansion model (P-BEM), and then the Kalman filter is employed to estimate and track the BEM coefficients by the detected data and pilot in each iteration. To reduce the effect of the error propagation on the channel estimation, the detection error is considered as part of the noise in the Kalman recursion in each iteration. Moreover, the employed Kalman filter does not include the estimated parameters of the AR model, so the proposed method has a fast convergence speed and it is more practical for the mobile MIMO-OFDM system.

This paper is organized as follows: Section II introduces the system model. Section III presents the proposed method in detail. The simulation results and conclusions are given in Section IV and V respectively.

The adopted notations are as follows: $diag\{\mathbf{x}\}$ is a diagonal matrix with $\mathbf{x}$ in its main diagonal, and $blckdiag\{\mathbf{A},\mathbf{B}\}$ is a block diagonal matrix with the matrices $\mathbf{A}$ and $\mathbf{B}$ on its main diagonal. $E\{\cdot\}$ and $\otimes$ are the expectation and Kronecker product operations respectively. $[\mathbf{X}]_{i,j}$ denotes the $(i,j)^{th}$ element of the matrix $\mathbf{X}$. $\mathbf{I}_N$ and $\mathbf{0}_N$ are the $N\times N$ identity matrix and the matrix of zeros respectively. $(\cdot)^H$, $(\cdot)^T$ and $(\cdot)^*$ stand respectively for Hermitian, transpose, and conjugate operations.

2. Signal Model

2.1 MIMO-OFDM System Model

Consider a MIMO-OFDM system with N_t transmit antennas and N_r receive antennas, and the duration of a MIMO-OFDM block is $T=N_sT_s$, where T_s is the sampling time and $N_s=N+N_c$, N and N_c are the number of the subcarriers and the length of the cyclic prefix (CP) respectively. Assume $\mathbf{x}_m$ is the m^{th} transmitted MIMO-OFDM block, and

$$\mathbf{x}_m = \left[\mathbf{x}_m^{(1)T},\ldots,\mathbf{x}_m^{(N_t)T}\right]^T \tag{1}$$

where $\mathbf{x}_m^{(t)}$ is the m^{th} transmitted OFDM symbol by the t^{th} transmit antenna, and

$\mathbf{x}_m^{(t)} = [x_{m,1}^{(t)}, ..., x_{m,N}^{(t)}]^T$, $x_{m,k}^{(t)}$ is the power-normalized information symbol sent by the t^{th} transmit antenna at the k^{th} subcarrier. After a multi-path Releigh channel, the m^{th} received MIMO-OFDM block can be written as

$$\mathbf{y}_m = \mathbf{H}_m \mathbf{x}_m + \mathbf{w}_m \tag{2}$$

where $\mathbf{y}_m = [\mathbf{y}_m^{(1)T}, ..., \mathbf{y}_m^{(N_r)T}]^T$, and $\mathbf{y}_m^{(r)} = [y_{m,1}^{(r)}, ..., y_{m,N}^{(r)}]^T$ is the m^{th} received OFDM symbol by the r^{th} receive antenna. $\mathbf{w}_m = [\mathbf{w}_m^{(1)T}, ..., \mathbf{w}_m^{(N_r)T}]^T$ is the $N_r N \times 1$ white complex Gaussian noise vector of covariance matrix $\sigma_w{}^2 \mathbf{I}_{NN_r}$, and $\mathbf{H}_m$ is a $N_r N \times N_t N$ MIMO channel matrix, i.e.,

$$\mathbf{H}_m = \begin{bmatrix} \mathbf{H}_m^{(1,1)} & \cdots & \mathbf{H}_m^{(1,N_t)} \\ \vdots & \ddots & \vdots \\ \mathbf{H}_m^{(N_r,1)} & \cdots & \mathbf{H}_m^{(N_r,N_t)} \end{bmatrix} \tag{3}$$

where $\mathbf{H}_m^{(r,t)}$ is the channel matrix between the t^{th} transmit antenna and r^{th} receive antenna. The entries of channel matrix $\mathbf{H}_m^{(r,t)}$ can be expressed as

$$\left[\mathbf{H}_m^{(r,t)}\right]_{i,i'} = \frac{1}{N} \sum_{l=0}^{L-1} e^{-\frac{j2\pi i' l}{N}} \sum_{n=0}^{N-1} \alpha_{l,m}^{(r,t)}(n) e^{\frac{j2\pi(i'-i)n}{N}} \tag{4}$$

where L is the number of the channel taps. $\alpha_{l,m}^{(r,t)}(n)$ is the n^{th} sampling of the l^{th} channel tap, which follows Jakes' power spectrum of the maximum Doppler frequency f_d, and $\alpha_{l,m}^{(r,t)}(n)$ is a zero mean complex Gaussian processes of variances $\sigma_{\alpha_l}^2$.

Define $\boldsymbol{\alpha}_{l,m}^{(r,t)} = [\alpha_{l,m}^{(r,t)}(0), ..., \alpha_{l,m}^{(r,t)}(N-1)]^T$, the correlation matrix of $\boldsymbol{\alpha}_{l,m}^{(r,t)}$ for the time-lag τ' is $\mathbf{R}_{\boldsymbol{\alpha}}^{(\tau')} = E\left\{\boldsymbol{\alpha}_{l,m}^{(r,t)} \boldsymbol{\alpha}_{l,m-\tau'}^{(r,t)\,H}\right\}$, and its element is given by

$$\left[\mathbf{R}_{\boldsymbol{\alpha}_l}^{(\tau')}\right]_{i,i'} = \sigma_{\alpha_l}^2 J_0\left(2\pi f_d T_s \left(i - i' + \tau' N_s\right)\right) \tag{5}$$

where $J_0(\cdot)$ is the zero-order Bessel function of the first kind.

2.2 BEM channel model

Since the number of the samples to estimate $N_t N_r LN$ is greater than the number of observation equations $N_r N$, it is not efficient to estimate the time-varying channel in (2), and it needs to reduce the number of the estimated parameters. Therefore, the channel coefficient $\alpha_{l,m}^{(r,t)}(n)$ is approximated by the BEM with the finite-parameters $c_{q,l,m}^{(r,t)}$ in the paper, and it is given as

$$\alpha_{l,m}^{(r,t)}(n) = \sum_{q=1}^{Q} b_{n,q} c_{q,l,m}^{(r,t)} + \zeta_{l,m}^{(r,t)}(n) \tag{6}$$

where $b_{n,q}$ is the basis function, and $\zeta_{l,m}^{(r,t)}(n)$ is the corresponding BEM modeling error, Q is the order of the BEM. To simplify notation, we rewrite the BEM in vector as

$$\boldsymbol{\alpha}_{l,m}^{(r,t)} = \mathbf{B}\mathbf{c}_{l,m}^{(r,t)} + \boldsymbol{\zeta}_{l,m}^{(r,t)} \tag{7}$$

where $[\mathbf{B}]_{n,q} = b_{n,q}$ is a matrix of size $N \times Q$, and

$$\mathbf{c}_{l,m}^{(r,t)} = \left[c_{1,l,m}^{(r,t)}, ..., c_{Q,l,m}^{(r,t)}\right]^T \tag{8}$$

$$\boldsymbol{\zeta}_{l,m}^{(r,t)} = \left[\zeta_{l,m}^{(r,t)}(0), ..., \zeta_{l,m}^{(r,t)}(N-1) \right]^T \tag{9}$$

The P-BEM based method is a simple channel modeling method without the accurate knowledge of the Doppler shift, and it is employed in the paper to model the time variation of the channel.

Using BEM in (7) and neglecting the BEM model error, the received OFDM symbol can be rewritten as

$$\mathbf{y}_m = \boldsymbol{\Gamma}_m \mathbf{c}_m + \mathbf{w}_m \tag{10}$$

where

$$\begin{aligned}
\mathbf{c}_m &= \left[\mathbf{c}_m^{(1,1)T}, ..., \mathbf{c}_m^{(1,N_t)T}, ..., \mathbf{c}_m^{(N_r,N_t)T} \right]^T \\
\mathbf{c}_m^{(r,t)} &= \left[\mathbf{c}_{0,m}^{(r,t)T}, ..., \mathbf{c}_{L-1,m}^{(r,t)\ T} \right]^T \\
\boldsymbol{\Gamma}_m &= \mathbf{I}_{N_r} \otimes \left[\boldsymbol{\Gamma}_m^{(1)}, ..., \boldsymbol{\Gamma}_m^{(N_t)} \right] \\
\boldsymbol{\Gamma}_m^{(t)} &= \frac{1}{N} \left[\mathbf{Z}_{0,m}^{(t)}, ..., \mathbf{Z}_{L-1,m}^{(t)} \right] \\
\mathbf{Z}_{l,m}^{(t)} &= \left[\mathbf{M}_1 diag\left\{ \mathbf{x}_m^{(t)} \right\} \mathbf{f}_l, ..., \mathbf{M}_Q diag\left\{ \mathbf{x}_m^{(t)} \right\} \mathbf{f}_l \right]
\end{aligned} \tag{11}$$

where $\mathbf{f}_l$ is the l^{th} column of the $N \times L$ Fourier matrix $\mathbf{F}$ and $\mathbf{M}_q$ is a $N \times N$ matrix, which are given by

$$\begin{aligned}
\left[\mathbf{F} \right]_{k,l} &= e^{-\frac{j2\pi kl}{N}}, l = 0, ..., L-1; k = 0, ..., N-1 \\
\left[\mathbf{M}_q \right]_{k,k'} &= \sum_{n=0}^{N-1} b_{n,q} e^{\frac{j2\pi(k'-k)n}{N}}, k = 0, ..., N-1; k' = 0, ..., N-1
\end{aligned} \tag{12}$$

Using the BEM coefficients, one can easily obtain $\mathbf{H}_m^{(r,t)}$ as

$$\mathbf{H}_m^{(r,t)} = \sum_{q=1}^{Q} \mathbf{M}_q diag\left\{ \mathbf{F} \boldsymbol{\chi}_{(q,m)}^{(r,t)} \right\} \tag{13}$$

where $\boldsymbol{\chi}_{(q,m)}^{(r,t)} = \left[c_{(q,1,m)}^{(r,t)}, ..., c_{(q,L,m)}^{(r,t)} \right]^T$.

3. Proposed Method

In the proposed method, the iterative algorithm for joint Kalman filter and data detection scheme is given to estimate the time-varying channel. Specifically, the Kalman filter is from the canonical state space model, which does not include the parameters of the AR model, and the detection error is considered as part of the noise in the Kalman filter to improve the estimation accuracy. In the following, the method is derived in detail.

3.1 Kalman Filter from Canonical State Space Model

Since the available schemes need to estimate the parameters of the AR model, it will take a large computation complexity. Moreover, the accuracy of the estimated parameters of the AR model will affect the convergence speed of the iterative scheme. Therefore, the proposed method employs a canonical state space model without the parameters of the AR model in

[12], which includes two parts, i.e., (a) the state equation consisting of the BEM coefficients and (b) the observation equation consisting of the pilot/ detected signal and the noise.

Define the state space model for the MIMO-OFDM system as $\mathbf{g}_m = \left[\mathbf{c}_m{}^T, ..., \mathbf{c}_{m-\rho+1}{}^T \right]^T$, where ρ is the size of the state vector. And then the state equation will be given as

$$\mathbf{g}_m = \mathbf{S}_1 \mathbf{g}_{m-1} + \mathbf{S}_2 \mathbf{u}_m \tag{14}$$

where $\mathbf{S}_1$ is the $\rho N_t N_r QL \times \rho N_t N_r QL$ state transition matrix, and it is given as

$$\mathbf{S}_1 = \begin{bmatrix} 0 & 0 & \cdots & \cdots & 0 & \cdots & 0 \\ \vdots & \vdots & \vdots & \vdots & \vdots & \vdots & \vdots \\ 0 & 0 & \cdots & \cdots & 0 & \cdots & 0 \\ 1 & 0 & \cdots & 0 & 0 & \vdots & \vdots \\ 0 & 1 & \cdots & 0 & 0 & \cdots & 0 \\ \vdots & \vdots & \ddots & \vdots & \vdots & \cdots & \vdots \\ 0 & 0 & \cdots & 1 & 0 & \cdots & 0 \end{bmatrix} \begin{matrix} \\ \\ \\ \\ \\ \\ \\ \end{matrix} \begin{matrix} \overbrace{\qquad\qquad\qquad\qquad\qquad\qquad}^{\rho N_t N_r QL} \\ \\ \\ \\ \\ \\ \\ \underbrace{\qquad\qquad}_{N_t N_r QL} \end{matrix} \begin{matrix} \\ \\ \\ \\ \\ \\ \\ \end{matrix} \begin{matrix} \left. \begin{matrix} \\ \\ \\ \\ \\ \\ \\ \end{matrix} \right\} N_t N_r QL \\ \\ \\ \\ \\ \\ \\ \left. \begin{matrix} \\ \\ \\ \\ \\ \\ \\ \end{matrix} \right\} \rho N_t N_r QL \end{matrix} \tag{15}$$

In (14), $\mathbf{S}_2 = \left[\mathbf{I}_{N_t N_r QL}, \mathbf{0}_{(\rho-1)N_t N_r QL \times N_t N_r QL} \right]^T$, and its dimension is $\rho N_t N_r QL \times N_t N_r QL$. $\mathbf{u}_m$ is the $N_t N_r QL \times 1$ vector, and $\mathbf{u}_m = \mathbf{c}_m$.

The observation equation can be expressed from (10) as

$$\mathbf{y}_m = \mathbf{S}_m \mathbf{g}_m + \mathbf{w}_m \tag{16}$$

where $\mathbf{S}_m = \left[\mathbf{\Gamma}_m, \mathbf{0}_{N_r N \times (\rho-1)N_t N_r QL} \right]$.

Using the Kalman filter for the state space model in (14) and (16), one can obtain as

---

Time update equations:

$$\begin{aligned} \hat{\mathbf{g}}_{m|m-1} &= \mathbf{S}_1 \hat{\mathbf{g}}_{m-1|m-1} \\ \mathbf{p}_{m|m-1} &= \mathbf{S}_1 \mathbf{p}_{m-1|m-1} \mathbf{S}_1{}^H + \mathbf{S}_2 \mathbf{C}_{\mathbf{u}_m} \mathbf{S}_2{}^H \end{aligned} \tag{17}$$

Measurement update equations:

$$\begin{aligned} \mathbf{K}_m &= \mathbf{p}_{m|m-1} \mathbf{S}_m{}^H \left(\mathbf{S}_m \mathbf{p}_{m|m-1} \mathbf{S}_m{}^H + \boldsymbol{\delta}^2 \right)^{-1} \\ \hat{\mathbf{g}}_{m|m} &= \hat{\mathbf{g}}_{m|m-1} + \mathbf{K}_m \left(\mathbf{y}_m - \mathbf{S}_m \hat{\mathbf{g}}_{m|m-1} \right) \\ \mathbf{p}_{m|m} &= \mathbf{p}_{m|m-1} - \mathbf{K}_m \mathbf{S}_m \mathbf{p}_{m|m-1} \\ \hat{\mathbf{c}}_m &= \mathbf{S}_2{}^H \hat{\mathbf{g}}_{m|m} \end{aligned} \tag{18}$$

---

where $\hat{\mathbf{g}}_{m|m-1}$ and $\hat{\mathbf{g}}_{m|m}$ are the priori and posteriori state estimate respectively. $\mathbf{p}_{m|m-1}$ and $\mathbf{p}_{m|m}$ are the priori and posteriori error estimate covariance matrix of size $\rho N_t N_r QL \times \rho N_t N_r QL$ respectively. In addition, $\hat{\mathbf{g}}_{0|0} = \mathbf{0}_{pLQN_r}$ and $\mathbf{p}_{0|0} = \mathbf{I}_{\rho N_t N_r QL \times \rho N_t N_r QL}$ are initiated. In (17), $\mathbf{C}_{\mathbf{u}_m}$ is the covariance matrix of $\mathbf{u}_m$, and

$$\mathbf{C}_{\mathbf{u}_m} = \mathbf{I}_{N_t N_r} \otimes blckdiag\left\{\mathbf{R}_{\mathbf{c}_0}^{(0)}, ..., \mathbf{R}_{\mathbf{c}_{L-1}}^{(0)}\right\} \tag{19}$$

where

$$\mathbf{R}_{\mathbf{c}_l}^{(0)} = E\left\{\mathbf{c}_{l,m}^{(r,t)}\mathbf{c}_{l,m}^{(r,t)H}\right\} = \left(\mathbf{B}^H\mathbf{B}\right)^{-1}\mathbf{B}^H\mathbf{R}_{\boldsymbol{\alpha}_l}^{(0)}\mathbf{B}\left(\mathbf{B}^H\mathbf{B}\right)^{-1} \tag{20}$$

In (18), $\boldsymbol{\delta}^2 = \sigma_w{}^2\mathbf{I}_{NN_r}$, and $\mathbf{K}_m$ is the Kalman gain.

3.2 Iterative algorithm for Joint Kalman Filter and Data Detection

To improve the accuracy of the channel estimation, the detected data along with pilots is employed. In one OFDM symbol, assume that N_p pilots subcarriers are evenly inserted into the N subcarriers. The algorithm proceeds as follows:

Initialization:

- $\hat{\mathbf{g}}_{0|0} = \mathbf{0}_{pN_tN_rLQ}$, $\mathbf{p}_{0|0} = \mathbf{I}_{\rho N_tN_rQL \times N_tN_rQL}$
- $m \leftarrow m+1$
- Execute the time update equations of Kalman filter in (17)
- Compute the channel matrix using (13)
- $i \leftarrow 1$

Recursion:

- Detection of the data symbol by using zero-forcing (ZF) equalizer
- Construct $\hat{\mathbf{S}}_m$ by the detected data and pilots
- Execute the measurement update equations of Kalman filter in (18)
- Compute the channel matrix using (13)
- $i \leftarrow i+1$

3.3 Iterative Algorithm considering Data Detection Error

In the iterative schemes, the error propagation caused by the data detection cannot be ignored and it will result in an error floor. To reduce the effect of the detection error on the channel estimation, the detection error will be considered as a part of the noise in the Kalman filter of the proposed method. Therefore, the covariance of the detection error needs to be given.

By [18], we divide the received signal in (16) into three parts, i.e., detected data, detection error and white noise, which is shown as

$$\begin{aligned}\mathbf{y}_m &= \hat{\mathbf{S}}_m\mathbf{g}_m + \left(\mathbf{S}_m - \hat{\mathbf{S}}_m\right)\mathbf{g}_m + \mathbf{w}_m \\ &= \hat{\mathbf{S}}_m\mathbf{g}_m + \boldsymbol{\psi}_m\end{aligned} \tag{21}$$

where $\hat{\mathbf{S}}_m$ is obtained by the pilots and detected data. $\boldsymbol{\psi}_m = \left(\mathbf{S}_m - \hat{\mathbf{S}}_m\right)\mathbf{g}_m + \mathbf{w}_m$ is the equivalent noise with zero mean. According to the derivation in Appendix, the covariance matrix of $\boldsymbol{\psi}_m$ is given by

$$\boldsymbol{\delta}_{\boldsymbol{\psi}_m} = \sigma_w^2\mathbf{I}_{NN_r} + \mathbf{I}_{N_r} \otimes \frac{1}{N^2}\sum_{t=1}^{N_t}\sum_{q_1,q_2=1}^{Q}\mathbf{M}_{q_1}\mathbf{v}_m^{(t)}\mathbf{M}_{q_2}^H\sum_{l=0}^{L-1}\left[\mathbf{R}_{\mathbf{c}_l}^{(0)}\right]_{q_1,q_2} \tag{22}$$

where

$$\mathbf{v}_m^{(t)} = diag\left\{\left[\left(v_{m,0}^{(t)}\right)^2, ..., \left(v_{m,N-1}^{(t)}\right)^2\right]\right\} \tag{23}$$

where $\left(v_{m,n}^{(t)}\right)^2$ is the variance of the detection error of the signal.

Using the state equation (14) and the observation model in (16), one can employ the Kalman filter to obtain the BEM coefficients, and $\boldsymbol{\delta}^2 = \boldsymbol{\delta}_{\boldsymbol{\psi}_m}$ in (18).

In (22), the variances $\left(v_{m,n}^{(t)}\right)^2, n = 0,..., N-1$ are needed for the calculation of the matrix $\boldsymbol{\delta}_{\boldsymbol{\psi}_m}$. Since $\left(v_{m,n}^{(t)}\right)^2$ =0 for the pilot, one only need to calculate the $\left(v_{m,n}^{(t)}\right)^2$ for the data symbol. To simplify the implementation of the Kalman filter, the expected value of $\left(v_{m,0}^{(t)}\right)^2$ is used to obtain the variance of the detection error of the data symbol by [18]. Then, one has

$$E\left\{\left(v_{m,0}^{(t)}\right)^2\right\} = E\left\{\left|x_{m,n}^{(t)}\right|^2\right\} - E\left\{\left|\hat{x}_{m,n}^{(t)}\right|^2\right\} = \sigma_x^2 - \sigma_{\hat{x}}^2 \tag{24}$$

where $\sigma_x^2 = 1$ since $x_{m,n}^{(t)}$ is the power-normalized symbol as we considered in section II, and $\hat{x}_{m,n}^{(t)}$ is the detected signal. Assuming that $\hat{x}_{m,n}^{(t)}$ is ergodic, one has

$$\sigma_{\hat{x}}^2 \approx \frac{1}{N_d M N_t} \sum_{t=1}^{N_t} \sum_{m=0}^{M-1} \sum_{n=0}^{N_d-1} \left|\hat{x}_{m,n}^{(t)}\right|^2 \tag{25}$$

where M is the number of OFDM symbols in one subframe, and N_d is the number of the data subcarriers during one OFDM duration. Then, the simplified estimator will consist in using an approximate covariance matrix of the equivalent noise $\boldsymbol{\psi}(m)$ in (21)

$$\begin{aligned} \boldsymbol{\delta}_{\boldsymbol{\psi}_m} &= \sigma_w^2 \mathbf{I}_{NN_r} + N_t\left(1-\sigma_{\hat{x}}^2\right)\mathbf{I}_{N_r} \\ &\otimes \frac{1}{N^2} \sum_{q_1,q_2=1}^{Q} \sum_{l=0}^{L-1} \left[\mathbf{R}_{\mathbf{c}_l}^{(0)}\right]_{q_1,q_2} \mathbf{M}_{q_1} diag\left\{\mathbf{1}_P\right\} \mathbf{M}_{q_2}^H \end{aligned} \tag{26}$$

where $\mathbf{1}_P$ is an $N \times 1$ vector composed of 0 at the pilot index, and 1 elsewhere.

Note that the type of the modulation affects the performance of the simplified covariance [18]. For the constant modulation (such as QPSK), $\left|x_{m,n}^{(t)}\right|$=1, so the first term of (24) $E\left\{\left(v_{m,0}^{(t)}\right)^2\right\}$ is equal to one, and the difference between the exact expression in (22) and approximate one in (26) is only the $\sigma_{\hat{x}}^2$. However, in the case of the non-constant modulation, the approximate covariance in (26) has more performance degradation due to the approximation of σ_x^2 and $\sigma_{\hat{x}}^2$.

3.4 Computation Complexity Analysis

In the section, the complexity of the proposed method and those of the conventional methods in [12][15][18] are compared. For the these algorithms, the main difference of the complexity focuses on the calculations of the matrices $\mathbf{S}_1$, $\mathbf{C}_{\mathbf{u}_m}$, and $\boldsymbol{\delta}^2$. In [12], since the matrix $\mathbf{S}_1$ is a constant matrix which only contains 0 and 1 and the data detection error is not considered, the computation complexity is focused on the calculation of the matrix $\mathbf{C}_{\mathbf{u}_m}$, which is about $2N_r^2N_t^2N_p$ floating-points (FLOPS). For the scheme in [15], since the data detection error is also not considered, the computation complexities caused by $\mathbf{S}_1$ and $\mathbf{C}_{\mathbf{u}_m}$ are respectively about $L[8NQ^2+2N^2Q+3Q^3+5o(Q^3)]$ FLOPS and $L[Q+2Q^3+o(Q^3)]$ FLOPS, where $o(Q^3)$ is the computation complexity of the matrix inversion for the $Q \times Q$ matrix. In [18], the computation complexities of $\mathbf{S}_1$ and $\mathbf{C}_{\mathbf{u}_m}$ are $L[8NQ^2+3N^2Q+4Q^3+7o(Q^3)]$ FLOPS, and

$L[4NQ^2+N^2Q+Q^3+2o(Q^3)]$ FLOPS respectively, and the complexity of $\boldsymbol{\delta}^2$ is about $2N[Q^2LN(8N-1)+3]$ FLOPS for the first iteration and the others is $6N$ FLOPS. In the proposed method, $\mathbf{S}_1$ is a constant matrix and composed of only 0 and 1 and it can be pre-computed and stored, the computation complexity of $\mathbf{C}_{\mathbf{u}_m}$ is about $L[4NQ^2+N^2Q+Q^3+2o(Q^3)]$ FLOPS. Since the detection error is considered in the proposed method, the complexity of its covariance matrix in $\boldsymbol{\delta}^2$ is about $2N[Q^2LN(8N-1)+3]$ FLOPS for the first iteration and the others is $6N$ FLOPS.

According to the above analysis, the comparison of the total computation complexity in one iteration for the different channel estimation methods is given in **Table 1**. From **Table 1**, one can see that the scheme in [12] has a lowest complexity due to its processing in frequency domain and it without considering the detection error. The computation complexity of the proposed method is lower than that of the scheme in [15] when the detection error is not considered, and the complexity will increase when the detection error is considered in the proposed method, but its performance will be greatly improved (which can be seen from the simulation results in section IV). Moreover, the increased complexity of the proposed method can be acceptably in the signal processing. Compared with the method in [18], the proposed method has a lower complexity since it does not need to estimate the parameters of the AR model and the covariance of the modeling error.

Table 1. The comparison of the computation complexity

Channel estimation method	Total computation complexity in one iteration
Ref.[12]	$2N_r^2N_t^2N_p$
Ref.[15]	$L[8NQ^2+2N^2Q+Q+5Q^3+6o(Q^3)]$
Ref.[18]	First iteration: $L[12NQ^2+3N^2Q+4Q^3+7o(Q^3)]+2N[Q^2LN(8N-1)+3]$ The other iterations: $L[12NQ^2+3N^2Q+4Q^3+7o(Q^3)]+6N$
Proposed method	First iteration: $L[4NQ^2+N^2Q+Q^3+2o(Q^3)]+2N[Q^2LN(8N-1)+3]$ The other iterations: $L[4NQ^2+N^2Q+Q^3+2o(Q^3)]+6N$

4. Simulation Results

To evaluate the performance of the proposed method, a MIMO-OFDM system with one transmit antenna and two receiver antennas is considered. The parameters of the system are as follows: the FFT size is 128, the CP length is chosen to be one-eighth of the FFT size, and the number of the pilots is 32 and the distance between two adjacent pilots is 4. The carrier frequency is 10GHz. The modulation scheme on the data subcarriers is QPSK. The vehicle speed is 300km/h, and the corresponding f_dT=0.2. ρ=2, where ρ is the size of the state vector. In the simulation, we assume Rayleigh uncorrelated fading condition from different transmitters to different receivers, which is considered to be a 6-tap channel with an exponentially decaying power delay profile specified by $exp(-l)$, where l is the tap index. The ZF equalizer is used in the simulation. In comparison with the proposed method, the algorithms in [12], [15] and [18] are also simulated.

To describe the convergence speed of the proposed algorithm, the convergence condition is that the hard decision after the current iteration is the same as that after the previous iteration in

the simulation. **Fig. 1** shows the average iterative numbers curve vs. SNRs. In **Fig. 1**, 'proposed accurate' is the proposed method with the accurate covariance of the detection error obtained by Eq. (22), and 'proposed approx' is the proposed method with the approximate covariance of the detection error obtained by Eq. (26). From **Fig. 1**, one can see that the iterative number decreases as the SNR increases, and the iterative number of the proposed approx is greater than that of the proposed accurate due to the error covariance approximation. Moreover, the maximum iterative number is less than 5 when the SNR is 0dB for both the proposed accurate and proposed approx, which indicates that the convergence speed of the proposed algorithm is relatively fast.

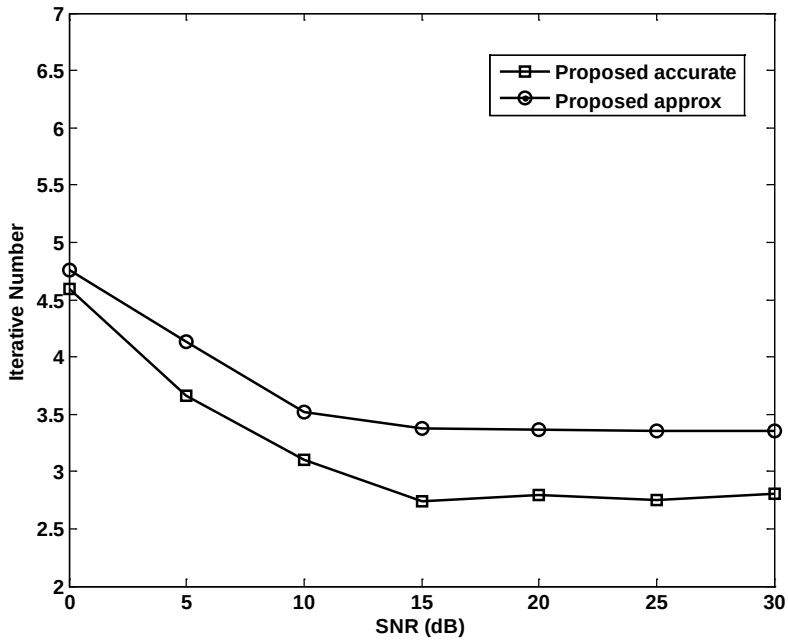

Fig. 1. Iterative numbers curve vs. SNRs for the proposed method with QPSK, f_dT=0.2 and N_p =32.

To further analyze the convergence of the proposed method, **Fig. 2** gives the mean square error (MSE) vs. iterative numbers in the different SNRs for the proposed method. In **Fig. 2**, we give the performance of the proposed method using different iterations, e.g., proposed approx-1 uses one iteration, and proposed approx-2 uses two iterations. 'All Data-aided' is the BEM-based Kalman filter estimation under the assumption that all the data is known at receiver. It can be seen that the MSE performance of the proposed method improves as the iterations increase, and the performance loss in the proposed approx is more obvious for the lower iterations and gradually decreases as the iterations increase. The MSE performance of the proposed approx using five iterations (proposed approx-5) is essentially coincident with that of the all data aided, and the proposed accurate using three iterations (proposed accurate-3) is essentially coincident with the all data aided. Moreover, when the iterations are greater than 5 and 3, the MSE performance of the proposed accurate and proposed approx are no longer significantly improved respectively, which can be seen proposed accurate-5 and proposed approx-7 in the figure.

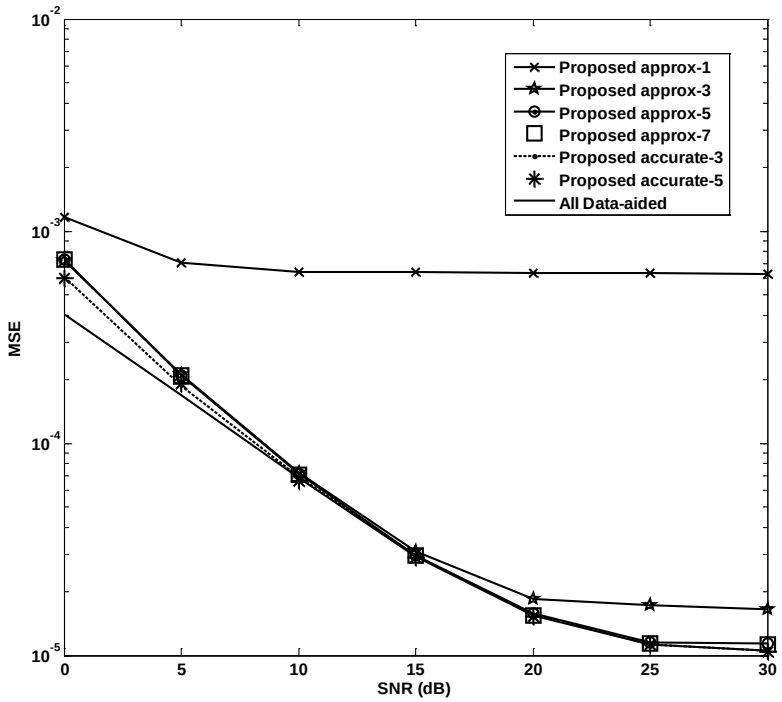

Fig. 2. MSE vs. iterative numbers in the different SNRs for the proposed method with QPSK, f_dT=0.2 and N_p =32.

To show the performance degradation of the proposed method with the approximate covariance matrix, we give the MSE performance of the proposed method with the accurate and approximate covariance of the detection error in **Fig. 3**. From **Fig. 3**, one can see that the propose accurate uses three iterations to approach to the performance of the all data aided, while the proposed approx needs five iterations due to the approximate value. Since the approximate value is relatively small, the difference of the iterative numbers between the proposed accurate and proposed approx is not large, which also can be seen from **Fig. 1**.

Fig. 4 and **Fig. 5** show the MSE and bit error rate (BER) performance for the different channel estimation methods respectively. It can be seen from the figures that the performance of the proposed method is better than those of the schemes in [12], [15] and [18] even when the iterative number is the same or not. The performance of the method in [12] is worst due to without considering the ICI caused by the time-varying channel and iteration processing. Since the data detection error is not considered for the iteration algorithm in [15], it needs more iterations and has a bad performance compared with the proposed method. In [18], the scheme needs to estimate the parameters of the AR model and the covariance of the modeling error, so it also need to more iterations to converge due to the effect of the estimation accuracy of these parameters. Moreover, the performance of the proposed method will be essentially coincident with that of the all data aided only by fewer iterations, such as three iterations for the proposed accurate and five iterations for the proposed approx.

Fig. 6 gives the MSE performance of the different channel estimation methods for f_dT=0.4 and N_p=32. It is shown that in comparison to **Fig. 4**, the MSE performance of the whole methods are deteriorated due to the Doppler shift increasing. In the case of the same iterations,

the performance of the proposed method is still better than those of the available schemes in [12], [15] and [18].

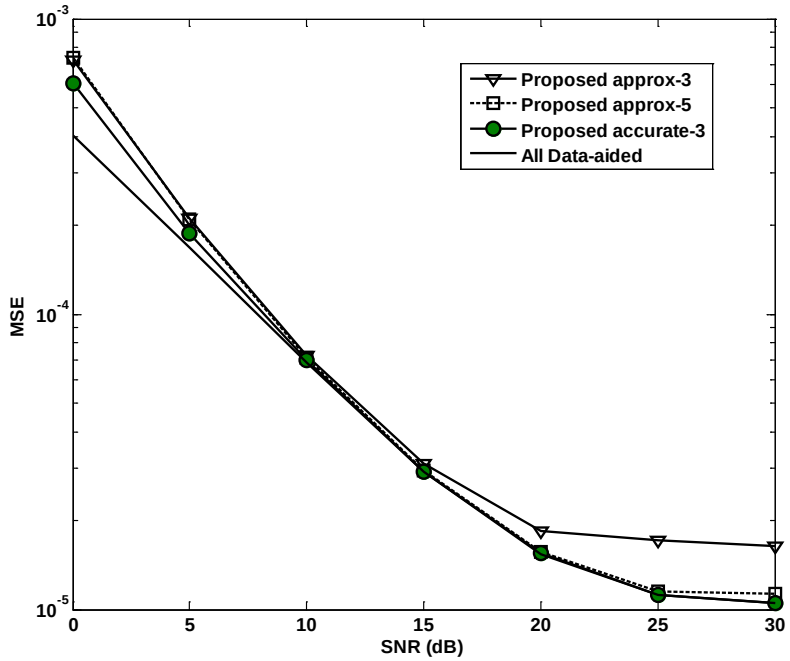

Fig. 3. MSE performance of the proposed method with accurate and approximate covariance of the detection error for QPSK, f_dT=0.2 and N_p =32.

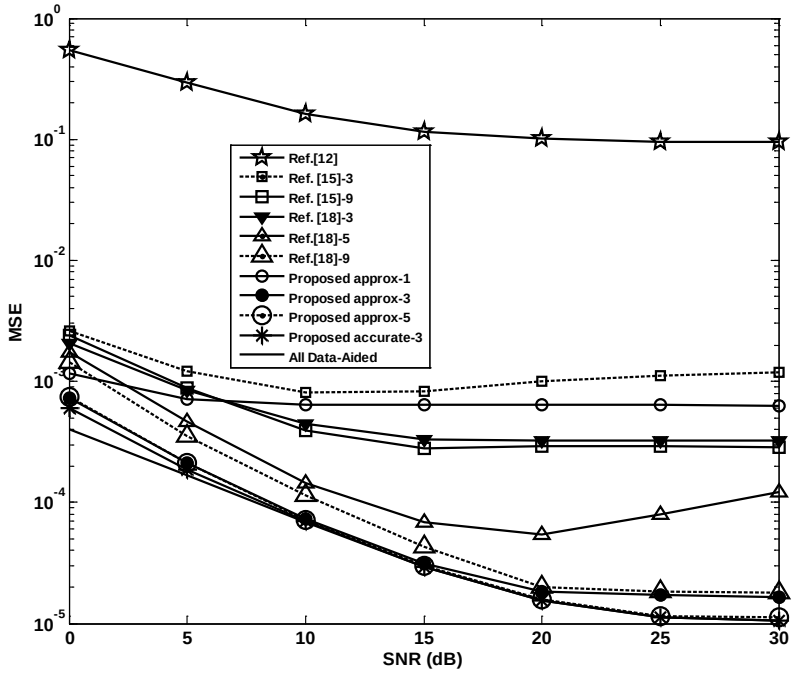

Fig. 4. MSE performance of the different channel estimation methods for QPSK, f_dT=0.2 and N_p =32.

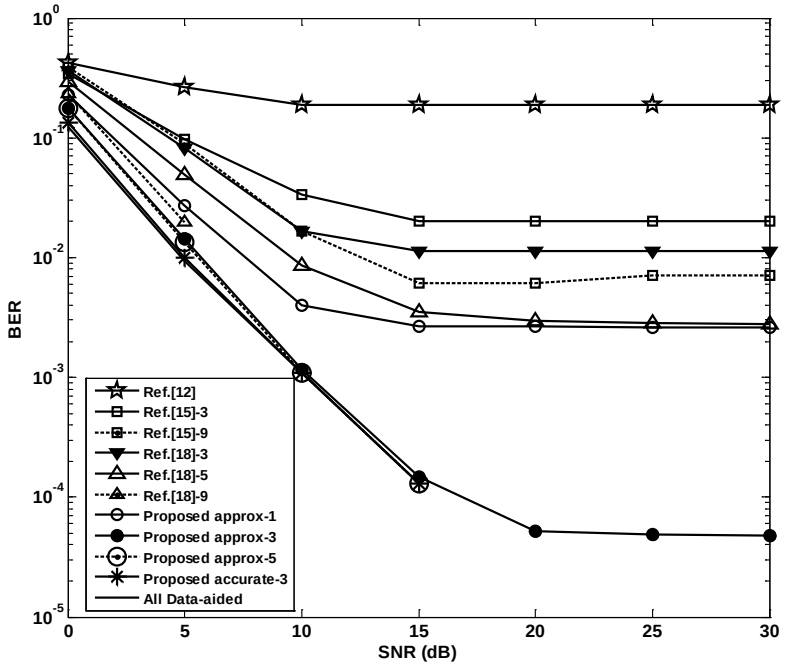

Fig. 5. BER performance of the system by using the different channel estimation methods for QPSK, f_dT=0.2 and N_p =32.

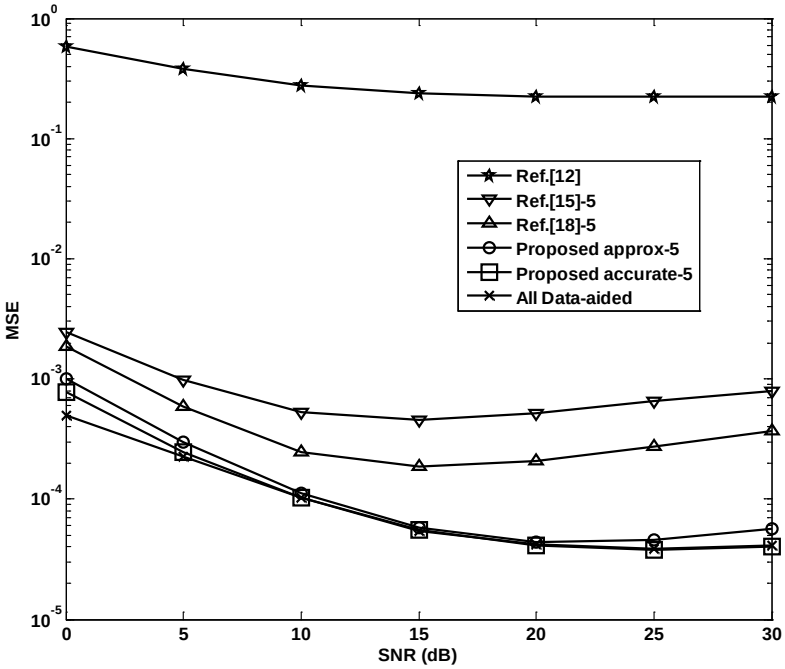

Fig. 6. MSE performance of the different channel estimation methods for QPSK, f_dT=0.4, N_p =32.

Fig. 7 shows the MSE performance of the different channel estimation methods for N_p=16 and f_dT=0.2. Compared with **Fig. 4**, the MSE performance of the whole methods are also deteriorated due to the pilots reducing. By the same iterations, the MSE performance of the proposed method is still better compared with the available schemes in [12], [15] and [18]. For the proposed approx with five iterations, there is a performance gap to the all data aided at the high SNRs, which rarely exists in the case of N_p=32 and f_dT =0.2 in **Fig. 4**. Compared with the case of f_dT =0.4 and N_p=32 in **Fig. 6**, one can find that the effect of the pilots reducing on the channel estimation is more serious than that of the Doppler shift increasing for the schemes in [12], [15] and [18] due to they without considering the detection error or the estimation accuracy of some parameters depends on the number of the pilots. Due to the detection error and the special Kalman filter employed in the proposed method, its performance in the case of the pilots reducing is better than that in case of the large Doppler shift.

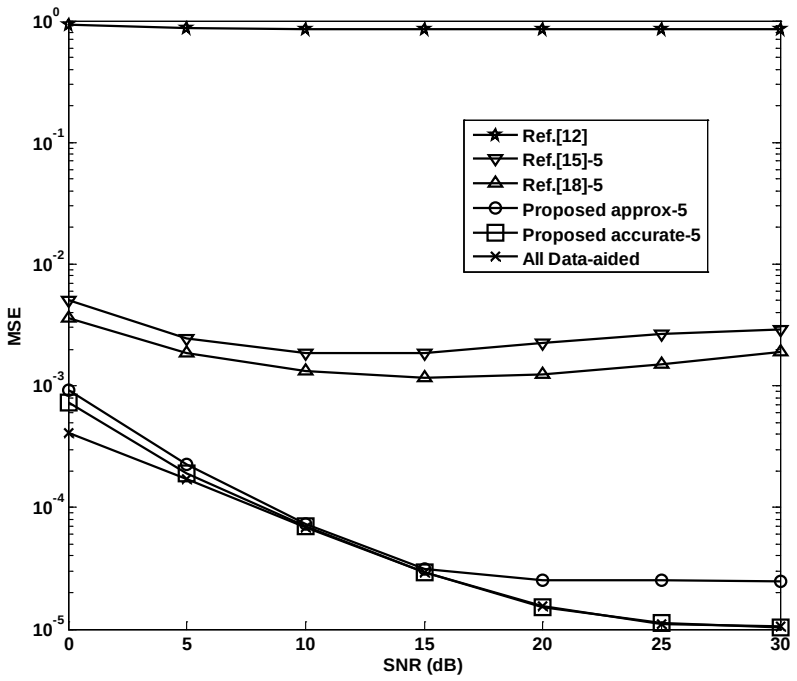

Fig. 7. MSE performance of the different channel estimation methods for QPSK, N_p=16, and f_dT=0.2.

To show the effect of the modulation type on the approximate proposed algorithm (proposed approx), the case of the non-constant modulation of 16QAM is also considered and it is shown in **Fig. 8**. Compared with the case of the constant modulation (QPSK) given in **Fig. 4**, the performance of the proposed approx is deteriorated due to the lower accuracy of the approximation in (26) for the non-constant modulation (16QAM), and it needs more iterations to tend to the all data aided. However, the performance of the proposed approx is still better than those of the available methods in [12], [15] and [18].

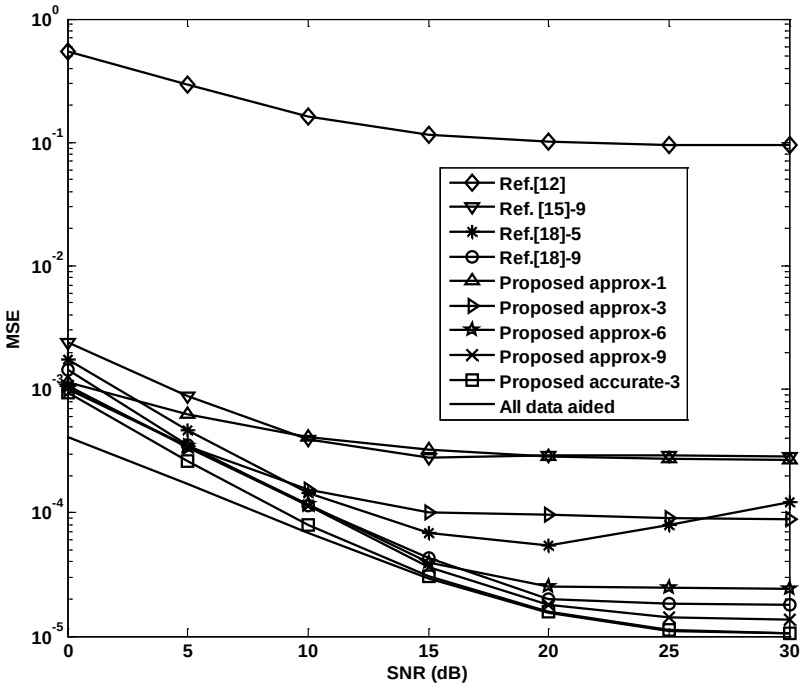

Fig. 8. MSE performance of the different channel estimation methods for 16QAM, f_dT=0.2, and N_p=32.

5. Conclusion

According to the high-speed mobile scenario, we proposed a practical time-varying channel estimation algorithm for the MIMO-OFDM system. Since the Kalman filter from the canonical state space model without the parameter of the AR model is employed and the data detection error is considered as part of the noise in the Kalman recursion, the proposed method is more practical compared with the available schemes. By the proposed method, the fast time-varying channel can be effectively estimated, and the proposed method can be used to estimate the channel in the high speed railway scenario. Moreover, the proposed method is not limited to the MIMO-OFDM system, and it can also be used in the SISO-OFDM or OFDMA system to improve the accuracy of the channel estimation.

Appendix

Define $\tilde{\mathbf{S}}_m = \mathbf{S}_m - \hat{\mathbf{S}}_m$, and then the equivalent noise $\boldsymbol{\psi}(m)$ can be rewritten as, whose autocorrelation matrix is

$$\begin{aligned} \boldsymbol{\delta}_{\boldsymbol{\psi}_m} &= E\left\{\boldsymbol{\psi}_m {\boldsymbol{\psi}_m}^H\right\} \\ &= E\left\{\left[\tilde{\mathbf{S}}_m \mathbf{g}_m + \mathbf{w}_m\right]\left[\tilde{\mathbf{S}}_m \mathbf{g}_m + \mathbf{w}_m\right]^H\right\} \end{aligned} \tag{27}$$

Since the noise has zero mean and is uncorrelated with the symbols, using (19) in (27), we obtain

$$\begin{aligned}\boldsymbol{\delta}_{\psi_m} &= E\left\{\mathbf{w}_m \mathbf{w}_m{}^H\right\} + E\left\{\tilde{\mathbf{S}}_m \mathbf{g}_m \mathbf{g}_m{}^H \tilde{\mathbf{S}}_m{}^H\right\} \\ &= \sigma_w^2 \mathbf{I}_{NN_r} + E\left\{\tilde{\mathbf{S}}_m \mathbf{g}_m \mathbf{g}_m{}^H \tilde{\mathbf{S}}_m{}^H\right\}\end{aligned} \tag{28}$$

In (28), the second term can be denoted as

$$\begin{aligned}\mathbf{E}_m &= E\left\{\tilde{\mathbf{S}}_m \mathbf{g}_m \mathbf{g}_m{}^H \tilde{\mathbf{S}}_m{}^H\right\} \\ &= E\left\{\tilde{\mathbf{S}}_m \mathbf{R}_{\mathbf{g}} \tilde{\mathbf{S}}_m{}^H\right\}\end{aligned} \tag{29}$$

where

$$\mathbf{R}_{\mathbf{g}} = \begin{bmatrix} \mathbf{R}_{\mathbf{g}}^{(0)} & \mathbf{R}_{\mathbf{g}}^{(1)} & \cdots & \mathbf{R}_{\mathbf{g}}^{(\rho-1)} \\ \mathbf{R}_{\mathbf{g}}^{(1)H} & \mathbf{R}_{\mathbf{g}}^{(0)} & \cdots & \mathbf{R}_{\mathbf{g}}^{(\rho-1)} \\ \vdots & \vdots & \ddots & \vdots \\ \mathbf{R}_{\mathbf{g}}^{(\rho-1)H} & \mathbf{R}_{\mathbf{g}}^{(\rho-2)H} & \cdots & \mathbf{R}_{\mathbf{g}}^{(0)} \end{bmatrix} \tag{30}$$

where

$$\mathbf{R}_{\mathbf{g}}^{(b)} = \mathbf{I}_{N_t N_r} \otimes \underbrace{blckdiag\left\{\mathbf{R}_{\mathbf{c}_0}^{(b)}, ..., \mathbf{R}_{\mathbf{c}_{L-1}}^{(b)}\right\}}_{\mathbf{R}_{\mathbf{c}}^{(b)}} \tag{31}$$

where

$$\mathbf{R}_{\mathbf{c}_l}^{(b)} = E\left\{\mathbf{c}_{l,m}^{(r,t)} \mathbf{c}_{l,m-b}^{(r,t)\,H}\right\} = \left(\mathbf{B}^H \mathbf{B}\right)^{-1} \mathbf{B}^H \mathbf{R}_{\boldsymbol{\alpha}_l}^{(b)} \mathbf{B} \left(\mathbf{B}^H \mathbf{B}\right)^{-1} \tag{32}$$

Since $\mathbf{S}_m = \left[\boldsymbol{\Gamma}_m, \mathbf{0}_{N_r N \times (\rho-1) N_t N_r QL}\right]$, Eq.(29) can be further expressed as

$$\begin{aligned}\mathbf{E}_m &= E\left\{\tilde{\mathbf{S}}_m \mathbf{R}_{\mathbf{g}} \tilde{\mathbf{S}}_m{}^H\right\} \\ &= E\left\{\tilde{\boldsymbol{\Gamma}}_m \mathbf{R}_{\mathbf{g}}^{(0)} \tilde{\boldsymbol{\Gamma}}_m{}^H\right\}\end{aligned} \tag{33}$$

Form (8), we can rewrite (33) as

$$\mathbf{E}_m = \mathbf{I}_{N_r} \otimes \sum_{t=1}^{N_t} \mathbf{E}_m^{(t)} \tag{34}$$

where

$$\begin{aligned}\mathbf{E}_m^{(t)} &= E\left\{\tilde{\boldsymbol{\Gamma}}_m^{(t)} \mathbf{R}_c^{(0)} \tilde{\boldsymbol{\Gamma}}_m^{(t)H}\right\} \\ &= \frac{1}{N^2} E\left\{\sum_{l=0}^{L-1} \tilde{\mathbf{Z}}_{l,m}^{(t)} \mathbf{R}_{\mathbf{c}_l}^{(0)} \tilde{\mathbf{Z}}_{l,m}^{(t)\,H}\right\}\end{aligned} \tag{35}$$

In (35), $\tilde{\mathbf{Z}}_{l,m}^{(t)}$ can obtained by $\tilde{\mathbf{x}}_m^{(t)}$, and $\tilde{\mathbf{x}}_m^{(t)}$ is the detection error. Using (8), one can obtain the element of $\mathbf{E}_m^{(t)}$ as

$$\begin{aligned}\left[\mathbf{E}_m^{(t)}\right]_{n,n'} = \frac{1}{N^2} \sum_{l=0}^{L-1} \sum_{q_1,q_2=1}^{Q} \sum_{n_1,n_2=0}^{N-1} &\left[\mathbf{M}_{q_1}\right]_{n,n_1} \left[\mathbf{M}_{q_2}{}^*\right]_{n',n_2} \\ &\times E\left\{\tilde{x}_{m,n_1}^{(t)} \tilde{x}_{m,n_2}^{(t)\,*}\right\} \left[\mathbf{F}\right]_{n_1,l} \left[\mathbf{F}^*\right]_{n_2,l} \left[\mathbf{R}_{\mathbf{c}_l}^{(0)}\right]_{q_1,q_2}\end{aligned} \tag{36}$$

Assuming that $\tilde{x}_{m,n}^{(t)}$ is uncorrelated with other symbols, which is justified by using a large

interleaver size, we obtain

$$E\left\{\tilde{x}_{m,n_1}^{(t)}\tilde{x}_{m,n_2}^{(t)\,*}\right\}=\begin{cases}\left(v_{m,n_1}^{(t)}\right)^2, n_1=n_2\\ 0, others\end{cases} \tag{37}$$

Therefore, (36) can be simplified as

$$\left[\mathbf{E}_m^{(t)}\right]_{n,n'}=\frac{1}{N^2}\sum_{q_1,q_2=1}^{Q}\sum_{n_1=0}^{N-1}\left(v_{m,n_1}^{(t)}\right)^2\left[\mathbf{M}_{q_1}\right]_{n,n_1}\left[\mathbf{M}_{q_2}^{\ *}\right]_{n',n_1}\sum_{l=0}^{L-1}\left[\mathbf{R}_{\mathbf{c}_l}^{(0)}\right]_{q_1,q_2} \tag{38}$$

Using (28) and (38), we can obtain $\boldsymbol{\delta}_{\boldsymbol{\psi}_m}$ as

$$\boldsymbol{\delta}_{\boldsymbol{\psi}_m}=\sigma_w^2\mathbf{I}_{NN_r}+\mathbf{I}_{N_r}\otimes\frac{1}{N^2}\sum_{t=1}^{N_t}\sum_{q_1,q_2=1}^{Q}\mathbf{M}_{q_1}\mathbf{v}_m^{(t)}\mathbf{M}_{q_2}^H\sum_{l=0}^{L-1}\left[\mathbf{R}_{\mathbf{c}_l}^{(0)}\right]_{q_1,q_2} \tag{39}$$

where $\mathbf{v}_m^{(t)}=diag\left\{\left[\left(v_{m,0}^{(t)}\right)^2,\ldots,\left(v_{m,N-1}^{(t)}\right)^2\right]\right\}$.

References

[1] Bölcskei H, Gesbert D, and Paulraj AJ, "On the Capacity of OFDM-Based Spatial Multiplexing Systems," *IEEE Transactions on Communications*, vol. 50, no. 2, pp. 225-234, 2002. Article (CrossRef Link)

[2] Najam Ul Hasan, Waleed Ejaz, Naveed Ejaz, "Network Selection and Channel Allocation for Spectrum Sharing in 5G Heterogeneous Networks," *IEEE Access*, vol. 4, pp. 980-992, 2016. Article (CrossRef Link)

[3] Wang ZL and Han Z, "A MIMO-OFDM Channel Estimation Approachn Using Time of Arrivals," *IEEE Transactions on Wireless Communications*, vol. 4, no. 3, pp. 1207-1213, 2005. Article (CrossRef Link)

[4] Li Y, "Simplified Channel Estimation for OFDM Systems with Multiple Transmit Antennas," *IEEE Transactions on Wireless Communications*, vol. 1, no. 1, pp. 67-75, 2002. Article (CrossRef Link)

[5] Wang ZJ, Zhu H, and Ray Liu KJ, "MIMO-OFDM Channel Estimation via Probabilistic Data Association Based TOAs," in *Proc of IEEE Global Communications Conference*, pp. 626-630, San Francisco, Dec. 1-5, 2003. Article (CrossRef Link)

[6] Wu JX, and Fan PZ, "A survey on high mobility wireless communications: Challenges, opportunities and solutions," *IEEE Access*, vol.4, pp. 450-476, 2016. Article (CrossRef Link)

[7] Ai B, Cheng X, Kürner T, "Challenges toward wireless communications for high-speed railway," *IEEE Transactions on Intelligent Transportation Systems*, vol. 15, no. 5, pp. 2143-2158, 2014. Article (CrossRef Link)

[8] Changkee Min, Namseok Chang, Jongsub Cha, "MIMO-OFDM downlink channel prediction for IEEE 802.16e systems using Kalman filter," in *Proc of WCNC 2007*, pp. 943-947, Kowloon, March 11-15, 2007. Article (CrossRef Link)

[9] Chen BS, Yang CY, and Liao WJ, "Robust Fast Time-Varying Multipath Fading Channel Estimation and Equalization for MIMO-OFDM Systems via a Fuzzy Method," *IEEE Transactions on Vehicular Technology*, vol. 61, no. 4, pp. 1599-1609, 2012. Article (CrossRef Link)

[10] Jihyung Kim, Byungjoon Park, and Daesik Hang, "Robust Channel Estimation in a mobile MIMO OFDM System," in *Proc of 2004 IEEE 59th Vehicular Technology Conference (VTC 2004-Spring)*, pp. 594-597, MILAN, May 17-19, 2004.Article (CrossRef Link)

[11] Zhao N, Yu FR, Sun HJ, Yin HX, Nallanathan A, Wang G, "Interference Alignment with Delayed Channel State Information and Dynamic AR-Model Channel Prediction in Wireless Networks," *Wireless Networks*, vol. 21, no. 4, pp. 1227-1242, 2015. Article (CrossRef Link)

[12] Takahiro NATORI, Nari TANABE, and Toshihiro FURUKAWA, "A MIMO-OFDM channel estimation algorithm for high-speed movement environments," in *Proc of ISCCP2014*, pp. 348-351, Athens, May 21-23, 2014.Article (CrossRef Link)
[13] Ren X, Tao MX, and Chen W, "Compressed Channel Estimation with Position-Based ICI Elimination for High-Mobility SIMO-OFDM Systems," *IEEE Transactions on Vehicular Technology*, no. 99, pp. 1-13,2015.Article (CrossRef Link)
[14] Wang GP, Gao FF, Chen W, and Tellambura C, "Channel Estimation and Training Design for Two-Way Relay Networks in Time-Selective Fading Environment," *IEEE Transactions on Wireless Communication*, vol. 10, no. 8, pp. 2681-2691, 2011. Article (CrossRef Link)
[15] Hijazi H, Simon EP and Ros L, "Channel estimation for MIMO-OFDM systems in fast time-varying environments," in *Proc. of 4th International Symposium on Communications, Control and Signal Processing* (*ISCCSP* 2010), pp. 3-5 Limassol, 2010. Article (CrossRef Link)
[16] Movahedian A, McGuire M, "Estimation of fast-fading channels for Turbo receivers with high-order modulation," *IEEE transactions on Vehicular Technology*, vol. 62, no. 2, pp. 667-678, 2013. Article (CrossRef Link)
[17] Zhao M, Shi Z, Reed CM, "Iterative Turbo channel estimation for OFDM system over Rapid dispersive fading channels," *IEEE Transactions on Wireless Communications*, vol. 7, no. 8, pp. 3174-3184, 2008. Article (CrossRef Link)
[18] Eric Pierre Simon, Mohammad Ali Khalighi, "Iterative soft-Kalman channel estimation for fast time-varying MIMO-OFDM channels," *IEEE wireless communication letters*, vol. 2, no. 6, pp. 599-602, 2013.Article (CrossRef Link)
[19] Yang LH, Ren GL, Yang BK and Qiu ZL, "Fast Time-Varying Channel Estimation Technique for LTE Uplink in HST Environment," *IEEE Transactions on Vehicular Technology*, vol. 61, no. 9, pp. 4009-4019, 2012. Article (CrossRef Link)
[20] Yang LH, Yang LX, Zhu HB, "Time varying channel estimation for SC-FDMA system under HST scenario," *Journal on Communications*, vol. 35, no. 9, pp. 91-98, 2014. Article (CrossRef Link)

Lihua Yang was born in Jiangsu, china in 1984. She received her B.S. degree in Electronics and communications engineering at Xi'an University of Science and Technology, 2007 and her M.S. degree in signal processing at Xidian University 2008. She received the Ph.D. degree in the communication and information systems at Xidian University on March 2013. She is currently a Lecturer of the College of Telecommunications and Information Engineering, Nanjing University of Posts and Telecommunications. Her research interests focus on the key technologies of the physical layer in the mobile wireless communications, and the network coding.

Longxiang Yang is with the College of Communications and Information Engineering, Nanjing University of Posts and Telecommunications (NJUPT), Nanjing, China. He is a full Professor and Doctoral Supervisor at NJUPT. His research interests span the broad area of wireless networks, cooperative communications and signal processing of communications. He has fulfilled multiple National Natural Science Foundations of China.

Yan Liang received the B.S. degree in Communications Engineering, M.S. and Ph.D. degrees in Communication and Information Systems from Nanjing University of Science & Technology in 2001, 2004 and 2013, respectively. From 2004–2008, she was with Lucent Technology as a research engineer. Since 2013, she has been a lecture in the College of Telecommunications and Information Engineering at Nanjing University of Posts and Telecommunications (NUPT), China. Her research interests include broadband wireless communication and communication signal processing.